

1 **The Role of Stratospheric Memory in Increased**
2 **Tropospheric NAM Persistence as Revealed by**
3 **Idealized Ensemble Forecasts**

E. P. Gerber

4 Center for Atmosphere Ocean Science, Courant Institute, New York

5 University, New York, New York USA

C. Orbe

6 Department of Applied Physics and Applied Mathematics, Columbia

7 University, New York, New York USA

L. M. Polvani

8 Department of Applied Physics and Applied Mathematics and Department

9 of Earth and Environmental Science, Columbia University, New York, New

10 York USA

E. P. Gerber, Center for Atmosphere Ocean Science, Courant Institute of Mathematical Sci-
ences, New York University, 251 Mercer St., New York NY 10012

C. Orbe, L. M. Polvani, Department of Applied Physics and Applied Mathematics, Columbia
University, 200 S. W. Mudd Building, MC 4701, 500 W. 120th Street, New York NY 10027

11 The coupling between the stratosphere and troposphere following Strato-
12 spheric Sudden Warming (SSW) events is investigated in an idealized atmo-
13 spheric General Circulation Model, with focus on the influence of stratospheric
14 memory on the troposphere. Ensemble forecasts are performed to confirm
15 the role of the stratosphere in the observed equatorward shift of the tropo-
16 spheric midlatitude jet following an SSW. It is demonstrated that the tro-
17 pospheric response to the weakening of the lower stratospheric vortex is ro-
18 bust, but weak in amplitude and thus easily masked by tropospheric vari-
19 ability. The amplitude of the response in the troposphere is crucially sensi-
20 tive to the depth of the SSW. The persistence of the response in the tropo-
21 sphere is attributed to both the increased predictability of the stratosphere
22 following an SSW, and the dynamical coupling between the tropospheric jet
23 and lower stratosphere. These results suggest value in resolving the strato-
24 sphere and assimilating upper atmospheric data in forecast models.

1. Introduction

25 The goal of this study is to investigate the coupling between the stratosphere and tro-
26 posphere following a Stratosphere Sudden Warming (SSW). By computing the Northern
27 Annular Mode (NAM) index on each pressure level independently, *Baldwin and Dunker-*
28 *ton* [2001] Found that SSWs tend to precede an equatorward shift of the tropospheric
29 midlatitude jet by roughly 10 days, and that the tropospheric anomalies, on average, per-
30 sist for two months. This coupling, however, is not entirely robust: some stratospheric
31 events “reach” the troposphere, but others produce little effect [*Baldwin and Dunkerton,*
32 2001, Fig. 1]. In addition, while the negative signal in the NAM appears to propagate
33 downward from the stratosphere, the direction of causality may not be so obvious; *Plumb*
34 *and Semeniuk* [2003] have shown in a stratosphere-only model that similar, seemingly
35 downward propagating signals can be driven exclusively by the lower boundary. As SSW
36 events are initiated by increased planetary wave fluxes from the troposphere [*Polvani and*
37 *Waugh*, 2004], it is possible that the dynamics driving the NAM response might also be
38 internal to the troposphere. This begs the question whether the stratospheric signal is
39 more of a distraction, that is, a passive player in a cycle entirely driven by tropospheric dy-
40 namics. To discount this possibility, we perform a series of ensemble forecast experiments
41 with an idealized General Circulation Model (GCM) to demonstrate the stratosphere’s
42 active role in maintaining the equatorward shift of the tropospheric jet.

43 Many earlier studies have probed stratosphere-troposphere coupling by perturbing the
44 stratosphere, and observing the resulting impact on the troposphere [e.g. *Boville*, 1984;
45 *Polvani and Kushner*, 2002; *Norton*, 2003; *Charlton et al.*, 2004; *Scaife et al.*, 2005]. Here

46 we apply a different approach, instead perturbing the *troposphere* around SSW events
47 to average away tropospheric internal variability, and so passively reveal the influence of
48 the stratosphere. Our strategy exploits the difference in time scales between the tropo-
49 sphere and the stratosphere [*Baldwin et al.*, 2003]. We launch a large ensemble forecast
50 before an SSW. Synoptic dynamics lead to rapid separation of ensemble members in the
51 troposphere, erasing any tropospheric memory. Provided the same SSW occurs in each
52 ensemble member, however, the stratosphere follows a more predictable trajectory due to
53 the slow recovery time scales of the lower stratosphere. This allows us to isolate a robust
54 signal in the troposphere as a direct response to stratospheric anomalies above.

55 Recent studies have explored the impact of the stratosphere on tropospheric predictabil-
56 ity in ensemble forecasts. Case studies with an operational forecast model show increased
57 predictability in both the stratosphere and the troposphere around the time of SSWs
58 [*Kuroda*, 2008; *Mukougawa et al.*, 2009]. *Marshall et al.* [2009] find enhanced predictabil-
59 ity in hindcasts where stratospheric initial conditions are included. Here we use an ide-
60 alized GCM that captures stratosphere-troposphere coupling with fidelity [*Gerber and*
61 *Polvani*, 2009], but with a computational efficiency that permits us to explore multiple
62 warming events with large ensembles. The model is idealized only in its forcing, inte-
63 grating the global primitive equations with horizontal and vertical resolutions comparable
64 to that of comprehensive GCMs. This allows us to focus exclusively on the dynamics of
65 stratosphere-troposphere coupling.

2. Methods

66 The atmospheric GCM used in this study integrates the dry primitive equations at T42
67 spectral resolution with 40 vertical levels extending to 0.7 Pa. It is run with perpetual
68 January conditions, maintained by Newtonian relaxation to a prescribed temperature
69 equilibrium profile and Rayleigh drag at the surface and upper boundary that approximate
70 surface friction and gravity wave drag, respectively, as described in detail by *Polvani and*
71 *Kushner* [2002]. The model is forced with a simple zonal wavenumber 2 topography of
72 maximum amplitude 3000 m, and the polar stratospheric vortex temperature is relaxed
73 to a profile with lapse rate $\gamma = 4$ K/km to produce realistic stratospheric coupling on
74 intraseasonal time scales. This is the configuration analyzed by *Gerber and Polvani* [2009],
75 and further details can be found therein.

76 A control integration of 10,000 days was run to produce a number of SSWs, identified
77 with the standard WMO criterion, i.e. the zonal mean zonal wind at 60° N and 10 hPa
78 reverses sign. From this integration, 4 events were selected with the intent to explore the
79 impact of differences in the initial tropospheric state (positive vs. negative NAM) and
80 depth of the warming. Around each of these events, 100 ensemble forecasts were created
81 by adding small, random perturbations to wavenumbers 4-10 of the vorticity field in the
82 Northern Hemisphere midlatitudes. The perturbations decay away from the surface as
83 $\exp[(p - p_s)^2/250^2]$, where pressure p is measured in hPa and p_s is the surface pressure,
84 and so are almost entirely confined to the troposphere.

The NAM at each pressure level is the first EOF of the daily zonal mean zonal wind,
weighted by the square root cosine of latitude. The NAM index is the area weighted
projection of the daily mean wind anomalies onto the EOF, and normalized to have unit

variance. The spread of the ensemble away from the control integration is quantified at each pressure level by the normalized mean square deviation,

$$\text{dev}_Z(p, t) = \frac{k_p}{2\pi^2} \int_0^{2\pi} \int_0^{\pi/2} \left(Z_{\text{ensb}}(\lambda, \phi, p, t) - Z_{\text{ctrl}}(\lambda, \phi, p, t) \right)^2 \cos \phi \, d\phi d\lambda, \quad (1)$$

85 here illustrated for the geopotential height Z . The subscripts ‘ensb’ and ‘ctrl’ refer to the
 86 ensemble member and control integrations, respectively, and λ and ϕ are longitude and
 87 latitude. The deviation $\text{dev}_Z(p, t)$ begins near zero for each ensemble member, the initial
 88 perturbation itself causing an imperceptible change. The (inverse of) the normalization
 89 constant, k_p^{-1} is set to twice the spatial mean of the variance of Z at each pressure level,
 90 so that $\text{dev}_Z(p, t)$ asymptotes to 1 for large t . More important for our purposes, when
 91 it reaches 1 the control and ensemble integrations are as statistically distinct as two
 92 independent realizations of the model, and thus all memory of the initial condition has
 93 been lost.

3. Results

94 Our ensemble forecast strategy is illustrated in Fig. 1. The solid black curve in the
 95 upper panels shows the strength of the zonal mean zonal wind at 60° N and 10 hPa in
 96 the control run around the time of a major warming, with day 0 corresponding to the
 97 minimum winds. In a series of initial experiments, ensemble forecast were launched 0, 10,
 98 20, ..., and 60 days before the warming (only 10 and 60 days are shown here). As one
 99 might expect, we find a threshold lead time, roughly 20 days in this model, beyond which
 100 the SSW ceases to be predictable: contrast the scatter of the green trajectories from an
 101 ensemble launched 60 days before the event (1a) to the red trajectories launched 10 days
 102 before the event (1b). We find that the stratosphere behaves qualitatively different after a

103 warming, with less spread in the trajectories that share a common warming event, as found
104 by [Mukougawa *et al.*, 2009] with an operational forecast model. The decreased spread
105 of the ensemble reveals an opportunity for extended predictability. As argued by *Gerber*
106 *and Polvani* [2009], the slow thermal relaxation time scales of the lower stratosphere in
107 part explain the slow recovery of the vortex. In addition, however, the weak winds above
108 the tropopause limit the propagation of planetary wave activity from the troposphere,
109 cutting off the dominant source of stratospheric variability.

110 In contrast, the overall predictability of the troposphere is not sensitive to the presence
111 or absence of a warming event. The lower panels of Fig. 1 show the normalized mean
112 square deviation of geopotential height dev_Z at 500 hPa. Quantitatively similar plots are
113 found in other tropospheric variables, e.g. surface pressure, geopotential height, and eddy
114 kinetic energy, at all levels below the tropopause. The perturbation variance initially
115 grows exponentially, approximately doubling every two days. Nonlinear effects become
116 important after one week, and the variance saturates after approximately three weeks. In
117 all cases, we find that the tropospheric circulations of the ensemble members are effectively
118 independent after 30 days. At this time, dev_Z has reached unity, indicating that the
119 perturbation “anomalies” are as large as the circulation itself and any memory of the
120 initial condition has been expunged from the flow.

121 Fig. 1 reveals a key separation in time scales between the troposphere and stratosphere.
122 Synoptic scale dynamics rapidly erase the initial condition in the troposphere [e.g. *Lorenz*,
123 1963]. Divergence of the tropospheric circulation then propagates upward into the strato-
124 sphere, in general leading to a loss of predictability after approximately one month – the

125 longer time scale set by slower divergence of the planetary waves in the troposphere, as
126 compared to the synoptic scale waves. After a major SSW, however, the stratospheric
127 circulation remains more predictable. We exploit this separation in time scales to couple
128 multiple realizations of the troposphere to the same stratospheric warming, essentially
129 allowing us to build a *Baldwin and Dunkerton* [2001] composite using a single event: 100
130 member ensembles are launched 10 days before 4 major warming events selected from the
131 control integration. The 10 day lead period ensures that all ensemble members experi-
132 ence the warming, but also allows the tropospheric circulation time to diverge before the
133 stratosphere recovers.

134 We first focus on the impact of tropospheric internal variability on stratosphere-
135 troposphere coupling. Fig. 2a shows the NAM index as a function of height and lag in
136 the control run for the event illustrated in Fig. 1b and d. For this event, the troposphere
137 is initially in a positive NAM state, and the stratospheric signal appears to propagate
138 downward approximately one month after the warming. Fig. 2b, however, illustrates an
139 ensemble member where the same stratospheric event appears unable to penetrate the
140 troposphere; if anything, the stratosphere in this integration experiences a stronger, more
141 persistent warming, but the troposphere fails to respond. Fig. 2c, in contrast, shows an
142 integration with a seemingly powerful response in the troposphere. The key difference
143 between the ensemble members is the internal variability of the troposphere. Only by
144 averaging over all ensemble members (Fig. 2d) can we see the “deterministic” response to
145 the stratospheric perturbation, a weak but significant response at long lags. On average,
146 it appears that the signal from the stratosphere penetrates to the troposphere after 10

147 days, as suggested by *Baldwin and Dunkerton* [2001], but here we focus on the long term
148 response, past 40 days, after which time all memory of the initial condition has been
149 erased in the troposphere. At these later times, one can be confident that the signal in
150 the troposphere must have been mediated by the stratosphere.

151 To quantify the variation across the entire ensemble, we focus on the tropospheric NAM
152 response averaged over days 40 through 90 in each ensemble member, as illustrated by
153 the boxes in Fig. 2. The first row of Table 1 shows the breakdown for the event shown in
154 Fig. 2: in 88 of 100 ensemble members, the NAM is negative over this period (as in Fig. 2a
155 and 2c) and only 12 times do we see a positive NAM (as in Fig. 2b). The probability of
156 randomly selecting 88 or more negative NAM events out of 100 randomly selected 50 day
157 periods is approximately $3e-14$, as shown in the last column of the table. Ensembles were
158 launched around three other SSW events in the control run, and the results are shown
159 lower in the table. We find that in all cases a negative response dominates the ensemble.
160 The NAM as a function of height and lag for the control run and the ensemble mean
161 composite of these other events are illustrated in Fig. 3.

162 Fig. 3 indicates that the variability in the tropospheric response depends both on the
163 depth of the stratospheric warming, and the initial conditions of the troposphere. Events
164 1 (Fig. 2a) and 3 (Fig. 3c) are both deep warmings. Here the signal penetrates to the
165 troposphere regardless of the tropospheric initial conditions. Events 2 and 4 (Fig. 3a,e)
166 were chosen because the initial warming (at day 0), did not penetrate as deeply in the
167 control run. In these cases, the signal in the troposphere is weaker, especially in case 4.

168 Figs. 2d and 3b, d, and f show *Baldwin and Dunkerton* [2001]-like composites for
169 a single event. Downward propagation from troposphere to stratosphere appears only
170 in events in which the tropospheric NAM is initially neutral or positive; otherwise the
171 response appears synchronous, as in Fig. 3d and f. As SSWs occur independently of the
172 initial state of the tropospheric NAM, half the time the troposphere will be in the positive
173 NAM state. In these cases, it takes on the order of 10-20 days, the e-folding timescale of
174 the tropospheric NAM, for the troposphere to adjust to the stratospheric perturbation,
175 producing the delay observed by *Baldwin and Dunkerton* [2001].

4. Discussion and Conclusions

176 We have demonstrated with a relatively simple model that the persistent equatorward
177 shift of the tropospheric jet stream following a Stratospheric Sudden Warming is mediated
178 through the stratosphere. The slow recovery of the polar vortex in the lowermost strato-
179 sphere following an SSW provides an additional source of memory for the troposphere,
180 leading to the persistent equatorward shift of the eddy driven jet. Thus, even though the
181 SSW is initially forced by wave activity from the troposphere [*Polvani and Waugh, 2004*],
182 the signal from the event is preserved in the stratosphere and is then able to influence
183 the troposphere at long lags. As seen from differences between the ensemble members,
184 internal tropospheric variability is large compared to the stratospheric influence, often
185 masking the stratospheric signal. The stratospheric influence can only be seen in com-
186 posites of multiple events [e.g. *Baldwin and Dunkerton, 2001*], or in ensemble composites
187 around a single event, as shown here.

188 Our experiments also suggest conditional limits to the predictability gain from the
189 stratosphere. As SSWs are driven by wave activity from the troposphere, their predictability
190 is limited by the chaotic nature of the troposphere. Once a warming has occurred, however,
191 there is hope for a mild increase in predictability on the long time scales of the lower
192 stratosphere. Furthermore, not all SSW events are created equal; a sharp reversal of the
193 zonal winds at 10 hPa does not guarantee deep penetration through the stratosphere, and
194 it is the lower stratosphere that appears to influence the troposphere.

195 The ability of our idealized model to capture stratosphere-troposphere coupling sug-
196 gests that the mechanism(s) behind the coupling lie in the primitive equation dynamics.
197 Two primary pathways for stratospheric influence have been identified: a direct, bal-
198 anced response to the stratospheric potential vorticity anomaly [e.g. *Hartley et al.*, 1998;
199 *Thompson et al.*, 2006], or influence of the lower stratospheric winds on tropospheric ed-
200 dies [e.g. *Wittman et al.*, 2004; *Song and Robinson*, 2004; *Chen and Zurita-Gotor*, 2008].
201 While our experiments cannot distinguish between these mechanisms, we have cemented
202 the role of the stratosphere in the tropospheric response to SSWs, despite the fact that
203 initial signal is forced from below, as noted by *Plumb and Semeniuk* [2003]. Our results
204 thus suggest the value of resolving the stratosphere and assimilating stratospheric data in
205 forecast models.

206 **Acknowledgments.** This work was funded, in part, by a grant from the National
207 Science Foundation to Columbia University. We also thank NCAR's computational and
208 Information Systems Laboratory, where integrations were performed.

References

- 209 Baldwin, M. P., and T. J. Dunkerton (2001), Stratospheric harbingers of anomalous
210 weather regimes, *Science*, *294*, 581–584.
- 211 Baldwin, M. P., D. B. Stephenson, D. W. J. Thompson, T. J. Dunkerton, A. J. Charl-
212 ton, and A. O’Neill (2003), Stratospheric memory and skill of extended-range weather
213 forecasts, *Science*, *301*, 636–640.
- 214 Boville, B. A. (1984), The influence of the polar night jet on the tropospheric circulation
215 in a GCM, *J. Atmos. Sci.*, *41*, 1132–1142.
- 216 Charlton, A. J., A. O’Neill, W. A. Lahoz, and A. C. Massacand (2004), Sensitivity of
217 tropospheric forecasts to stratospheric initial conditions, *Quart. J. Roy. Meteor. Soc.*,
218 *130*, 1771–1792.
- 219 Chen, G., and P. Zurita-Gotor (2008), The tropospheric jet response to prescribed zonal
220 forcing in an idealized atmospheric model, *J. Atmos. Sci.*, *65*, 2254–2271.
- 221 Gerber, E. P., and L. M. Polvani (2009), Stratosphere-troposphere coupling in a relatively
222 simple AGCM: The importance of stratospheric variability, *J. Climate*, *22*, 1920–1933.
- 223 Hartley, D. E., J. T. Villarín, R. X. Black, and C. A. Davis (1998), A new perspective on
224 the dynamical link between the stratosphere and troposphere, *Nature*, *391*, 471–474.
- 225 Jung, T., J. Barkmeijer, M. Leutbecher, T. Palmer, M. Rodwell, and F. Vitart (2009),
226 On the role of the stratosphere in medium-range and extended-range forecasting, *EGU*
227 *General Assembly*, *11*, EGU2009–13,575–1.
- 228 Kuroda, Y. (2008), Role of the stratosphere on the predictability of medium-range
229 weather: A case study of winter 2003–2004, *Geophys. Res. Lett.*, *35*, L19,701,

- 230 doi:10.1029/2008GL034,902.
- 231 Lorenz, E. N. (1963), Deterministic nonperiodic flow, *J. Atmos. Sci.*, *20*, 130–141.
- 232 Marshall, A. G., A. A. Scaife, and S. Ineson (2009), Enhanced seasonal prediction of
233 European winter warming following volcanic eruptions, *J. Climate*, *in press*.
- 234 Mukougawa, H., T. Hirooka, and Y. Kuroda (2009), Influence of stratospheric circulation
235 on the predictability of the tropospheric Northern Annular Mode, *Geophys. Res. Lett.*,
236 *36*, L08,814, doi:10.1029/2008GL037,127.
- 237 Norton, W. A. (2003), Sensitivity of Northern Hemisphere surface climate to sim-
238 ulation of the stratospheric polar vortex, *Geophys. Res. Lett.*, *30* (12), 1627,
239 doi:10.1029/2003GL016,958.
- 240 Plumb, R. A., and K. Semeniuk (2003), Downward migration of extratropical zonal wind
241 anomalies, *J. Geophys. Res.*, *108*(D7), 4223, doi: 2002JD002,773.
- 242 Polvani, L. M., and P. J. Kushner (2002), Tropospheric response to stratospheric per-
243 turbations in a relatively simple general circulation model, *Geophys. Res. Lett.*, *29*(7),
244 10.1029/2001GL014,284.
- 245 Polvani, L. M., and D. W. Waugh (2004), Upward wave activity flux as a precursor to
246 extreme stratospheric events and subsequent anomalous surface weather regimes, *J.*
247 *Climate*, *17*, 3548–3554.
- 248 Scaife, A. A., J. R. Knight, G. K. Vallis, and C. K. Folland (2005), A stratospheric
249 influence on the winter nao and North Atlantic surface climate, *Geophys. Res. Lett.*, *32*,
250 L18,715, doi:10.1029/2005GL023,226.

251 Song, Y., and W. A. Robinson (2004), Dynamical mechanisms for stratospheric influences
252 on the troposphere, *J. Atmos. Sci.*, *61*, 1711–1725.

253 Thompson, D. W. J., J. C. Furtado, and T. G. Shepherd (2006), On the tropospheric
254 response to anomalous stratospheric wave drag and radiative heating, *J. Atmos. Sci.*,
255 *63*, 2616–2629.

256 Wittman, M. A. H., L. M. Polvani, R. K. Scott, and A. J. Charlton (2004), Stratospheric
257 influence on baroclinic lifecycles and its connection to the Artic Oscillation, *Geophys.*
258 *Res. Lett.*, *31*, L16,113, doi:10.1029/2004GL020,503.

Table 1. The tropospheric NAM response in the ensemble SSW forecasts. Column 2 lists the tropospheric NAM state at the SSW onset, columns 3 and 4: the number of instances the tropospheric NAM is negative or positive, averaged over the last 50 days of the integration (40-90 days after the SSW event), and column 5: the ratio between them. The probabilities in column 6 show the chances of randomly obtaining a distribution this biased (or more so) in 100 randomly chosen 50 day intervals from the control run.

event	initial state	Negative	Positive	Ratio	Probability
1	positive	88	12	7.3	3.1e-14
2	positive	71	29	2.4	1.1e-4
3	negative	78	22	3.5	1.0e-7
4	negative	59	41	1.4	0.11

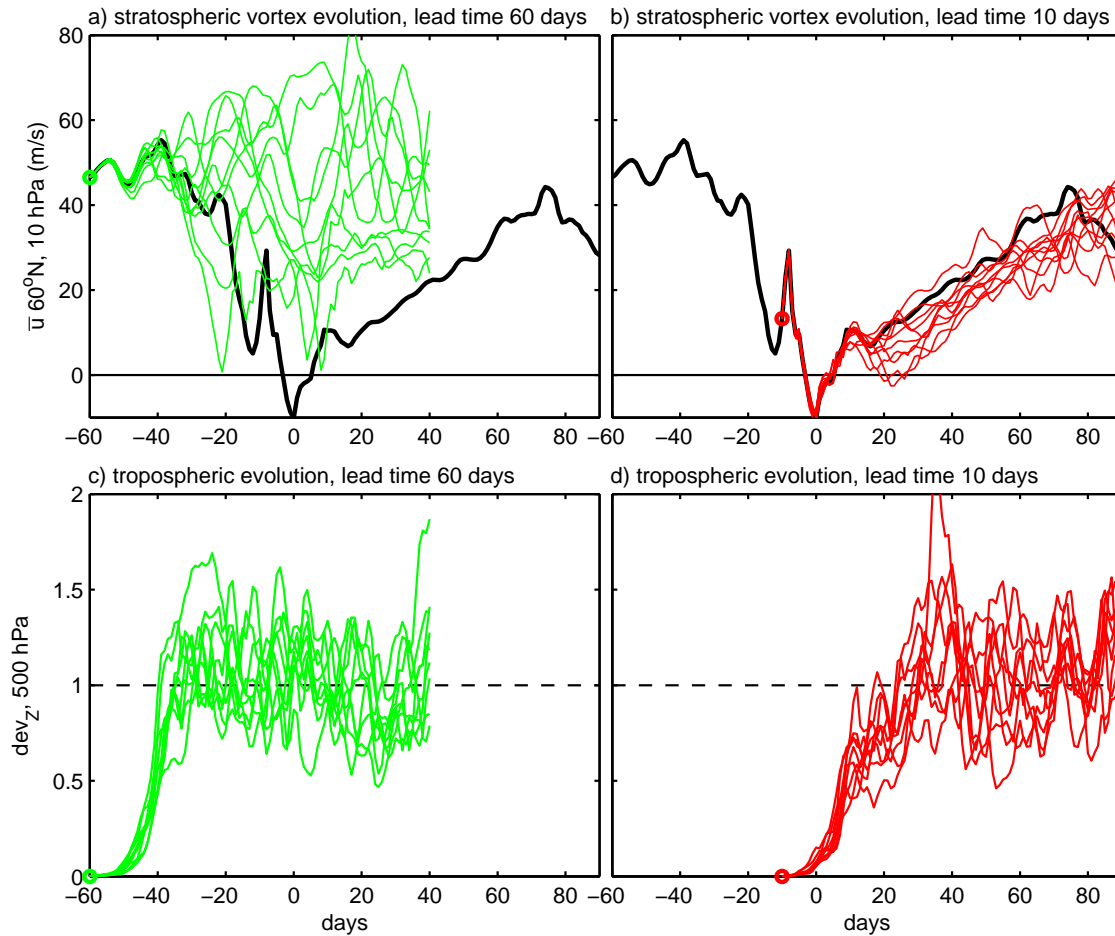


Figure 1. The ensemble forecast strategy, illustrated for SSW event 1. At top, the strength of the stratospheric vortex is quantified by the winds at 60°N and 10 hPa. The control is marked by the black curve, and ensemble members launched (left) 60 days and (right) 10 days are marked by green and red curves, respectively. At bottom, the spread of ensemble trajectories away from the control in the troposphere is quantified by the normalized mean square deviation, dev_Z , at 500 hPa for the same two forecast experiments. Note the similarity in tropospheric spread in the two ensembles, in contrast to the difference in spread in the stratosphere.

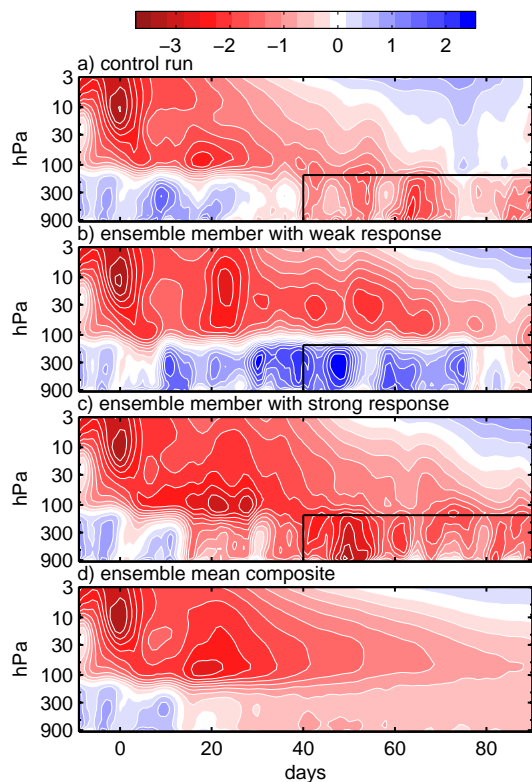


Figure 2. The NAM index as a function of pressure and time for (a) the control integration, (b) an ensemble member with seemingly no tropospheric response, (c) an ensemble member with a strong downward signal, and (d) the ensemble mean composite, averaged for 100 integrations. The plots are based on event 1, the forecast experiment illustrated in Fig. 1b and d, and day 0 marks the SSW onset. The sign of the tropospheric response listed in Table 1 is determined from the NAM index in the black boxes in the lower right corners.

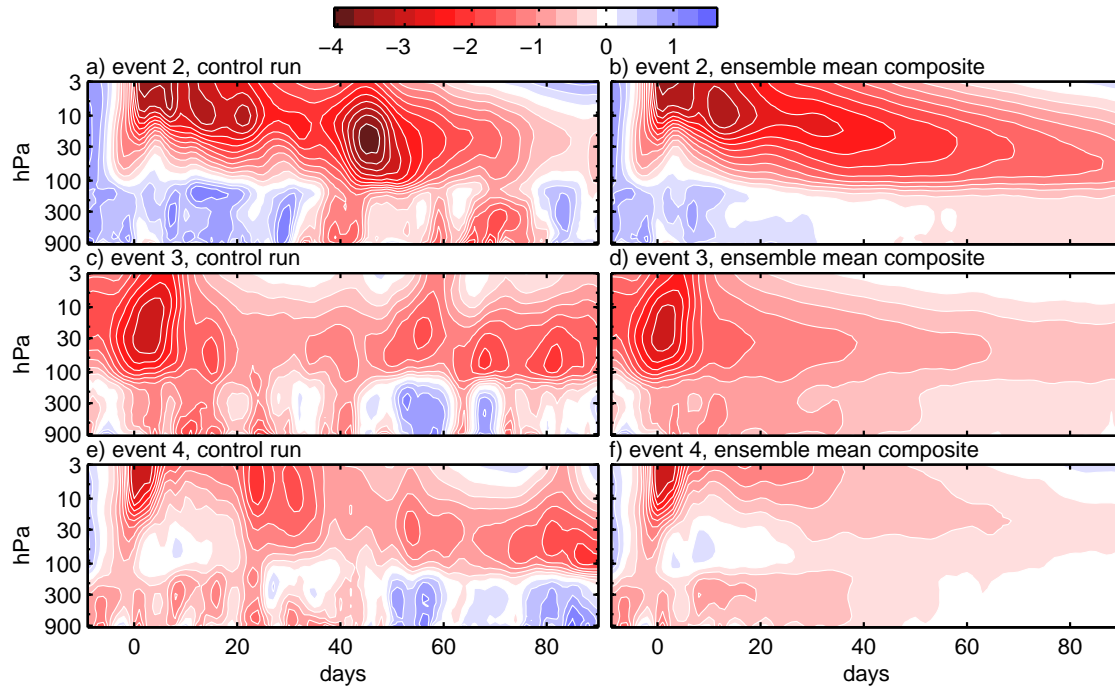


Figure 3. The NAM index as a function of pressure and time in the (left) control integration and (right) ensemble mean composite for SSW events 2, 3, and 4. These plots are to be compared with those in Fig. 2a and d, for event 1.